Cytoplasmic lipid droplet accumulation in developing mammary epithelial cells: roles of adipophilin and lipid metabolism

Tanya D. Russell,[1,*,†] Carol A. Palmer,[1,§] David J. Orlicky,[**] Andreas Fischer,[††] Michael C. Rudolph,[§] Margaret C. Neville,[†,§,§§] and James L. McManaman[2,*,†,§,§§]

Graduate Programs in Molecular Biology* and Cell and Developmental Biology,[§§] Division of Basic Reproductive Science, Department of Obstetrics and Gynecology,[†] and Departments of Physiology and Biophysics[§] and Pathology,** University of Colorado Health Sciences Center, Aurora, CO; and Department of Pharmacology and Toxicology,[††] Charité-University Medicine, Berlin, Germany

Abstract PAT proteins (perilipin, adipophilin, and TIP47) are hypothesized to be critical regulators of lipid accumulation in eukaryotic cells. We investigated the developmental relationships between the expression of these proteins and cytoplasmic lipid droplet (CLD) accumulation in differentiating secretory epithelial cells in mouse mammary glands. Adipophilin (ADPH) specifically localized to CLD in differentiating and lactating mammary glands and was found exclusively in the secreted lipid droplet fraction of mouse milk. ADPH transcripts were selectively detected in secretory epithelial cells, and steady-state levels of both ADPH mRNA and protein increased during secretory differentiation in patterns consistent with functional linkage to CLD accumulation. TIP47 also was detected in secretory epithelial cells; however, it had a diffuse punctate appearance, and its mRNA and protein expression patterns did not correlate with CLD accumulation. Perilipin-positive adipose cells and steady-state levels of perilipin mRNA and protein decreased during mammary gland differentiation, suggesting a progressive loss of adipose lipid storage during this process. Collectively, these data demonstrate that increased ADPH expression is a specialized property of differentiated secretory epithelial cells and provide developmental evidence specifically linking increased ADPH expression to increased CLD accumulation. In addition, evidence is presented that the epithelial and adipose compartments of the mammary gland undergo concerted, developmentally regulated shifts in lipid metabolism that increase the availability of fatty acids necessary for lipid synthesis by milk-secreting cells.— Russell, T. D., C. A. Palmer, D. J. Orlicky, A. Fischer, M. C. Rudolph, M. C. Neville, and J. L. McManaman. **Cytoplasmic lipid droplet accumulation in developing mammary epithelial cells: roles of adipophilin and lipid metabolism. *J. Lipid Res.* 2007.** 48: **1463–1475.**

Supplementary key words perilipin • mammary gland • adipose • fatty acid • cytoplasmic lipid droplet • differentiation • triglyceride

Lipids are a key constituent of milk, providing a large proportion of neonatal calories and essential fatty acids required for membrane synthesis. In many species, the lactating mammary gland is among the most active lipogenic organs in the body (1, 2). Functional differentiation of the mammary gland occurs during pregnancy with the formation and growth of alveoli, which are the milk-secreting units of the mammary gland (3, 4). Alveoli are composed of a single layer of secretory epithelial cells that actively synthesize and secrete proteins, sugars, and lipids into milk (5). Unlike milk proteins and sugars, which are secreted by classical secretory vesicle pathways (5), milk lipids are secreted by a unique membrane envelopment process (5, 6). Milk lipids originate from triglyceride and cholesteryl esters, which are synthesized by enzymes located on the endoplasmic reticulum and are released as protein-coated cytoplasmic lipid droplets (CLDs) (5). For secretion into milk, CLDs contact and become progressively enveloped by the apical plasma membrane (6, 7) before being released into the lumina of mammary alveoli as membrane-coated structures known as milk fat globules (MFGs). Despite the nutritional importance of milk lipids and the prominence of lipid biogenesis and secretion to the function of alveolar epithelial cells, the factors regulating the formation and secretion of CLDs remain poorly defined.

The PAT (for perilipin, adipophilin, and TIP47) family of lipid droplet-associated proteins is thought to play a key role in regulating the formation and secretion of CLDs (5, 8–10). Although perilipin has limited tissue expression (9, 11–15), adipophilin (ADPH) and TIP47 are thought to be expressed ubiquitously (16–18). TIP47 was coincidentally discovered as a placenta-specific gene known as the

Manuscript received 26 October 2006 and in revised form 15 March 2007.
Published, JLR Papers in Press, April 23, 2007.
DOI 10.1194/jlr.M600474-JLR200

[1] T. D. Russell and C. A. Palmer contributed equally to these studies.
[2] To whom correspondence should be addressed.
e-mail: jim.mcmanaman@uchsc.edu

48 kDa placental protein 17b, or PP17b (19, 20), as well as an endocytic vesicle-trafficking protein (21). Subsequently, others speculated that TIP47 may also localize to lipid droplets (10, 22). Cellular levels of ADPH have been shown to correlate with lipid accumulation in a variety of cells and tissues (23–29). This protein localizes to CLD in many mammalian cell types, including mammary epithelial cells, and is hypothesized to play a key role in CLD formation (16, 17, 30, 31). Furthermore, recent studies showing that exogenous expression of ADPH can increase CLD and triacylglycerol accumulation in cell culture models provide direct evidence that ADPH can modulate CLD levels (32–34). Previous studies in our laboratory demonstrating that ADPH forms a stable complex with xanthine oxidoreductase and butyrophilin (35), two proteins critically required for milk lipid secretion (36, 37), implicate ADPH in both the formation and secretion of CLDs. However, evidence linking ADPH expression to CLD formation in the mammary gland is lacking, and possible contributions of other PAT proteins to these processes have not been investigated.

Histological studies (7) demonstrated that CLDs begin to accumulate in the secretory epithelium of the mouse mammary gland during the last half of pregnancy, in conjunction with the differentiation of alveoli; however, the mechanisms regulating this accumulation have not been defined. Cell culture studies have demonstrated that ADPH mRNA levels increase in differentiating adipocytes (16), and previous studies have shown that ADPH localizes to CLDs in differentiating mouse mammary glands (2). However, ADPH expression in the developing mammary gland has not been examined, and it is unclear to what extent ADPH expression is related to CLD accumulation during mammary gland differentiation or whether other PAT proteins are involved. In this study, we define the localization and developmental relationships between PAT protein expression and CLD accumulation in the differentiating mouse mammary gland. Our results indicate that CLD accumulation in differentiating secretory epithelial cells is a sequentially ordered process initiated by increased ADPH expression and is developmentally linked to increased fatty acid availability attributable to the activation of lipid synthesis gene expression in the secretory epithelium and reduced lipid storage in mammary adipose tissue.

MATERIALS AND METHODS

Antibodies

Guinea pig polyclonal antibodies to perilipin were obtained commercially (Research Diagnostics Incorporated/Fitzgerald Industries International, Flanders, NJ). Antibodies to the N-terminal 25 amino acid sequence of murine ADPH were generated in rabbits and affinity-purified (Affinity Bioreagents, Golden, CO) or obtained commercially (Research Diagnostics/Fitzgerald Industries). Antibodies to the N-terminal 16 amino acids of murine TIP47 were generated in rabbits (Affinity Bioreagents). Rabbit antibodies to perilipin were obtained commercially (Research Diagnostics/Fitzgerald Industries). The specificities of ADPH and TIP47 antibodies were established by competition assays using specific immunizing peptides in both Western blot and immunofluorescence assays and by the absence of reaction of anti-ADPH and anti-TIP47 with purified recombinant mouse TIP47 and mouse ADPH proteins, respectively (data not shown).

Animals and tissue preparation

CD-1 mice (Charles River, Inc., Wilmington, MA) were maintained as breeding colonies at the Animal Resource Center of the University of Colorado Health Sciences Center (UCHSC) and housed individually. Pregnancy was timed by the observation of vaginal plugs after mating. The first day of pregnancy is taken as the day of vaginal plug detection. Parturition occurs on approximately day 19 of pregnancy and is also designated day 1 of lactation. Mammary tissue was removed from animals euthanized by carbon dioxide at the times indicated below and frozen in liquid nitrogen or processed for immunofluorescence microscopy (35). All animal procedures were approved by the Institutional Animal Care and Use Committee of the UCHSC.

Protein extraction and MFG isolation

Mammary tissue was ground under liquid nitrogen using a mortar and pestle. Ground tissue was suspended in lysis buffer (150 mM NaCl, 50 mM Tris, pH 7.0, 0.1% Triton X-100, 1 μg/ml protease inhibitor, 5 mM sodium orthovanadate, and 50 mM sodium fluoride). Tissue was spun at 3,000 *g* for 10 min at 4°C. Supernatant was subjected to methanol/chloroform extraction (38). The pellet was rinsed with methanol, dried, and suspended in 10% SDS solution. Protein concentrations were determined by the Micro BCA method (Pierce, Rockford, IL).

Whole and skim milk were collected as described previously (39) from continuously bred primiparous and multiparous mice milked on day 10 of lactation. MFGs were isolated from fresh milk by flotation through sucrose (40). Briefly, milk was adjusted to 10% sucrose, overlaid with 2 volumes of PBS, and centrifuged at 5,000 rpm for 20 min in a clinical centrifuge at 4°C. The top MFG layer was carefully removed and the process was repeated. The tube was frozen on dry ice, and the MFG fraction was excised and stored at −80°C before assay.

Immunoblot analysis

Proteins (50 μg) from mammary gland extracts or MFGs were separated on 10% polyacrylamide gels, transferred to nitrocellulose membranes, and probed with primary antibodies at the following concentrations: rabbit or guinea pig anti-ADPH, 1:1,000; rabbit anti-TIP47, 1:2,000; rabbit anti-perilipin, 1:2,000. Corresponding horseradish peroxidase-conjugated secondary antibodies (Sigma Chemical Co., St. Louis, MO) were used according to the manufacturer's specifications. Western Lightening Chemiluminescence Reagent (Perkin-Elmer, Boston, MA) was used to detect bands, and band intensities were quantified by densitometry (ChemiDoc system; Bio-Rad Laboratories, Hercules, CA). Preliminary studies were performed to verify that the densitometry responses of each protein were in the linear range. Each tissue was analyzed at least twice with similar results.

Isolation and quantitation of mRNA

Total RNA was extracted from frozen tissue or cultured cells using Trizol (Life Technologies, Gaithersburg, MD) according to the manufacturer's instructions. The purity, concentration, and integrity of total RNA were verified using a NanoDrop spectrophotometer (NanoDrop Technologies, Wilmington, DE) and

the RNA 6000 Nano Assay (Agilent Technologies, Palo Alto, CA) at the UCHSC Cancer Core. Random primed reverse transcription was carried out on 30 ng of total RNA as described previously (35). Perilipin A mRNA was quantified by semiquantitative RT-PCR on an Applied Biosystems 310 Genetic Analyzer using the primer pairs indicated in **Table 1**. mRNA values were expressed relative to the levels of mouse β-actin mRNA. Sizes and amounts of the PCR products were calculated using GeneScan software (Perkin-Elmer Applied Biosystems, Foster City, CA). Control experiments were performed to optimize signal linearity. Oligonucleotide primers for perilipin and β-actin were synthesized by the Department of Biochemistry and Molecular Biology at the University of New Mexico, and the fluorescent nucleotide tags were obtained from Perkin-Elmer Applied Biosystems.

ADPH and TIP47 transcript copy numbers were determined by quantitative real-time PCR (QRT-PCR) analysis using a multiplexing strategy to provide an internal standard for normalization (β-2-microglobulin). Similar results were obtained if copy number values were normalized to total input RNA (data not shown). Primers, probes, and amplicons used in these experiments are listed in Table 1. PCR was carried out on 96-well plates using the following combination of reagents: a master mix including 12.5 μl of PCR mix (Perkin-Elmer Applied Biosystems), 2.5 μl of ADPH or TIP47 primer/probe solution, 2.5 μl of β-2-microglobulin primer/probe solution, 0.25 μl of 100 U/μl AmpErase-UNG, 0.125 μl of 50 U/μl AmpliTaqGold polymerase, and 3.85 μl of nuclease-free water (Perkin-Elmer Applied Biosystems). QRT-PCR data were captured using an Opticon Monitor II real-time PCR detection system using the accompanying software version 2.02.24 (Bio-Rad Laboratories). Copy numbers of the investigated genes and the internal β-2-microglobulin were calculated from the respective amplicon standard curves using the formula $10^{[(\text{cycle time} - \text{Y intercept})/(\text{slope})]}$. Tissues at each time point were analyzed at least twice with similar results.

In situ hybridization

In situ hybridization was performed on 5 μm paraffin sections of paraformaldehyde-fixed mammary gland, prepared by overnight incubation of freshly dissected mammary tissue in neutral buffered formalin before embedding in paraffin. Sense and antisense probes to mouse ADPH were labeled with digoxigenin using the DIG RNA Labeling Kit (Roche Applied Science, Indianapolis, IN) according to the manufacturer's instructions. Antisense probes were generated from SP6 polymerase transcripts of the *Hind*III-digested pcDNA vector containing a full-length mouse ADPH insert (pADPH[FL]) (33). Sense probes were generated from T7 transcripts of the *Xho*I-digested pADPH. To obtain 200–300 bp fragments, the labeled transcripts were incubated in hydrolysis buffer (10 mM DTT, 80 mM $NaHCO_3$, and 120 mM Na_2CO_3) for 25 min at 65°C, and the reaction was stopped on ice by the addition of an equal volume of stop solution (10 mM DTT, 1% acetic acid, and 100 mM sodium acetate). Labeled probes were then stored at −80°C until used.

Sections were deparaffinized in xylene and rehydrated in graded alcohols, postfixed in 4% paraformaldehyde, and digested with 10 μg/ml proteinase K in a buffer containing 20 mM Tris and 1 mM EDTA for 10 min. After a second postfixation in 4% paraformaldehyde, the sections were washed twice in PBS and 2× SSC and incubated at room temperature in Tris-Glycine buffer (100 mM Tris and 45 mM glycine, pH 7.0) for 30 min and then with hybridization buffer [50% formamide, 5× Denhardt's solution, 200 μg/ml yeast tRNA (Sigma Chemical Co.), and 100 μg/ml sonicated salmon sperm DNA] for 4 h at room temperature. After addition of the labeled probes, hybridization was performed overnight at 72°C. Posthybridization washes were carried out in 50% formamide and 1% Tween 20 in 2× SSC at 65°C followed by two washes in MABT (100 mM malic acid, 150 mM NaCl, and 1% Tween 20) for 30 min each at room temperature. Slides were then blocked in MABT containing 1% blocking reagent (Boehringer Mannheim, Indianapolis, IN) and 10% normal sheep serum (Jackson ImmunoResearch Laboratories, Inc., West Grove, PA) for 1 h at room temperature and incubated in a 1:100 dilution of alkaline phosphatase-coupled sheep anti-digoxigenin antibody (Roche Applied Science) overnight at 4°C. After three 30 min washes in MABT at room temperature, the sections were equilibrated in 100 mM Tris, pH 9.5, 100 mM NaCl, and 5 mM MgCl for 5 min and then incubated with BM Purple alkaline phosphatase substrate (Roche Applied Science) for 1–6 h at room temperature as indicated. The reaction was stopped by briefly rinsing in PBS, and the sections were mounted in Permount and analyzed by light microscopy using a Leitz microscope equipped with a Kodak 290 digital camera.

TABLE 1. Primer list for RT-PCR and QRT-PCR

Assay	Gene	Primers and Probes
RT-PCR	Perilipin	5′-TET™– CAA GGG CCC AAC CCT G 3′–CGG AGG CGG GTA GAG ATG G
	β-actin	5′-6-FAM™– AGC AGC CGT GGC CAT CTC TTG CTC GAA GTC 3′- AAC CGC GAG AAG ATG ACC CAG ATC ATG TTT
QRT-PCR	ADPH	Forward: 5′-CAG CCA ACG TCC GAG ATT G-3′ Reverse: 5′-CAC ATC CTT CGC CCC AGT T-3′ Probe: 5′-FAM/TGC CAG TGC CAG AGG TGC CG-3′ Amplicon: 5′-CAG CCA ACG TCC GAG ATT GTT GCC AGT GCC AGA GGT GCC GTA ACT GGG GCG AAG GAT GTG-3′
	TIP47	Forward: 5′-CTC AAG CTG CTA TGG AGG ACC C-3′ Reverse: 5′-CAT ACG TGG AAC TGA TAA GAG GCA-3′ Probe: 5′56/FAM/CGT GGT GGA TCG TGT TGC CGG/36-TAMSp-3′ Amplicon: 5′-AAC TCA AGC TGC TAT GGA GGA ACC TGT TGT GCA GCC CAG CGT GGT GGA TCG TGT TGC CGG CCT GCC TCT TAT CAG TTC CAC GTA TGA A-3′
	B2- Microglobulin	Forward: 5′-GAT CAC ATG TCT CGA TCC CAG TAG-3′ Reverse: 5′-CAT ACG CCT GCA GAG TTA AGC A-3′ Probe: 5′-Hex/AGT ATG GCC GAG CCC GAG ACC G-3′ Amplicon: 5′-AAC ATA CGC CTG CAG AGT TAA GCA TGC CAG TAT GGC CGA GCC CAA GAC CGT CTA CTG GGA TCG AGA CAT GTG ATC AA-3′

In situ hybridization analyses of mammary tissue were repeated at least twice with similar results.

Microarray analysis

Total RNA was acquired, verified as described above, amplified, biotin-labeled (Enzo, Farmingdale, NY), and fragmented according to the 2002 protocol for eukaryotic target preparation (Affymetrix, Santa Clara, CA). Acceptable samples were hybridized to Affymetrix Mu74Av2 microarray chips. Raw data were gathered from scanned array chips using Affymetrix Microarray Suite version 5.0. Quality control chip statistics were evaluated from each array, including background intensity, noise, scaling factor, 3′–5′ ratios of the "housekeeping" genes, percentage distribution of calls, and the presence of "spiked" control genes. Compiled data in the form of 28 individual CEL files, the primary output of scanned Mu74Av2 microarray chips using the contemporary GeneChip Operating Software version 1.1 (Affymetrix), were imported to GeneSpring (Silicon Genetics, Redwood City, CA) for analysis using the native probe level GC-Robust Multi-Array Average algorithm. The complete results of this analysis are available at http://www.ncbi.nlm.nih.gov/geo under the series record GSE4222.

Data analysis

Genes were removed that scored <15.0 RAW intensity data units in four or more of the conditions analyzed. Genes that were expressed within 15% of their mean across all time points were also removed, giving a filtered list of 6,560 genes. To define genes that vary significantly over either the time course or the diet experiment, the Kruskal-Wallis nonparametric statistical test was run on the 6,560 gene list using a false discovery rate of 0.05.

Immunofluorescence microscopy

Freshly dissected mouse mammary tissue was fixed by overnight incubation in 4% paraformaldehyde in neutral buffered saline and embedded in paraffin at the UCHSC Pathology Core facility. Microtome sections (8 μm) were mounted on glass slides, deparaffinized and hydrated, and subjected to antigen retrieval (Vector Laboratories, Burlingame, CA) as described (35). The sections were then permeabilized in 0.2% glycine in PBS and blocked with 5% normal goat serum and 0.1% (w/v) saponin in PBS overnight at 4°C. Perilipin, ADPH, and TIP47 were immunolabeled with the appropriate antibodies (1:100 for perilipin and ADPH, 1:200 for TIP47) for 1 h at room temperature. The sections were then rinsed in PBS and incubated with a solution of Cy3-labeled donkey anti-rabbit IgG (Jackson ImmunoResearch Laboratories) or Alexa Fluor® 594-labeled donkey anti-rabbit IgG (Invitrogen/Molecular Probes, Carlsbad, CA) containing 4 μl/ml Alexa Fluor® 488 conjugate of wheat germ agglutinin (Invitrogen/Molecular Probes) and 0.03 μg/ml 4′,6-diamidino-2-phenylindole (Sigma Chemical Co.) in PBS for 45 min, rinsed with PBS, and mounted. Cultured cells were fixed in 3.7% formalin, washed in PBS, extracted with methyl alcohol at −20°C, and stained for ADPH and nuclei as described above.

Image analysis and CLD quantitation

Immunofluorescence images were captured at room temperature on a Nikon Diaphot fluorescence microscope equipped with a Cooke SensiCam charge-coupled device camera (Tonawand, NY) using Slidebook software (Intelligent Imaging Innovations, Inc., Denver, CO) as described previously (35). All images were digitally deconvolved using the No Neighbors algorithm (Slidebook), converted to TIFF files, and processed by Photoshop (Adobe Systems, Inc., Mountain View, CA). Average CLD diameters were determined by analysis of individual CLDs in 30–60 randomly chosen alveoli from three sections per animal. Three animals were analyzed per time point. Individual CLDs were enumerated using the masking functions of Slidebook. A lower limit of 200 nm was used in quantifying CLDs, because structures below this size were not adequately resolved.

Statistical analysis

Statistical significance was determined using Student's *t*-test.

RESULTS

ADPH is the PAT protein on CLDs in mouse mammary epithelial cells and MFGs

ADPH is a prominent surface-associated protein of CLDs in epithelial cells of bovine and mouse mammary glands (16, 17, 30) and a major protein constituent of the membrane surrounding MFGs in milk of mice and cattle (30, 35, 41). Recent studies have also suggested that TIP47 can associate with CLDs and MFGs (22, 42). To determine which PAT proteins are associated with CLDs in milk-producing mammary epithelial cells of the mouse, we compared the localizations of ADPH, TIP47, and perilipin in mammary glands of fully lactating mice. During lactation, the mammary gland is composed mainly of a system of ducts connected to terminal alveoli, which are responsible for synthesizing and secreting milk. Alveoli are composed of a single layer of secretory epithelial cells surrounding a central lumen. **Figure 1A** shows immunofluorescence staining of ADPH, TIP47, and perilipin in cross-sections of CD1 mouse mammary glands taken at lactation day 10 (panels a–c). Corresponding differential interference contrast images of each section (Fig. 1A, panels d–f) are shown below the fluorescence images to illustrate the relationships between fluorescence staining and structural features of the mammary tissue. The immunofluorescence images in Fig. 1A show that ADPH, TIP47, and perilipin differ in their cellular and subcellular localization patterns. ADPH localized exclusively to CLD within secretory epithelial cells of mammary alveoli and to secreted MFGs in alveolar lumens (Fig. 1A, panel a). TIP47 was also found in secretory epithelial cells, but in contrast to ADPH, it exhibited a diffusely distributed punctate staining pattern and did not appear to be associated with CLDs or MFGs (Fig. 1A, panel b). Furthermore, we found TIP47 but not ADPH staining in mammary adipose cells (Fig. 1A, arrow). In agreement with the known localization of perilipin to lipid droplets in adipose tissue (9, 11, 13, 43, 44), perilipin staining was restricted to a few small islands of lipid-depleted adipose tissue that remain in the mammary gland during lactation. Immunoblot analysis of mouse milk fractions showed that ADPH staining was restricted to MFGs, whereas TIP47 immunoreactivity was found only in the skim (fat-depleted) milk fraction (Fig. 1B). Consistent with its adipose localization, perilipin was not detected in milk (data not shown). These results indicate that ADPH is the only PAT protein asso-

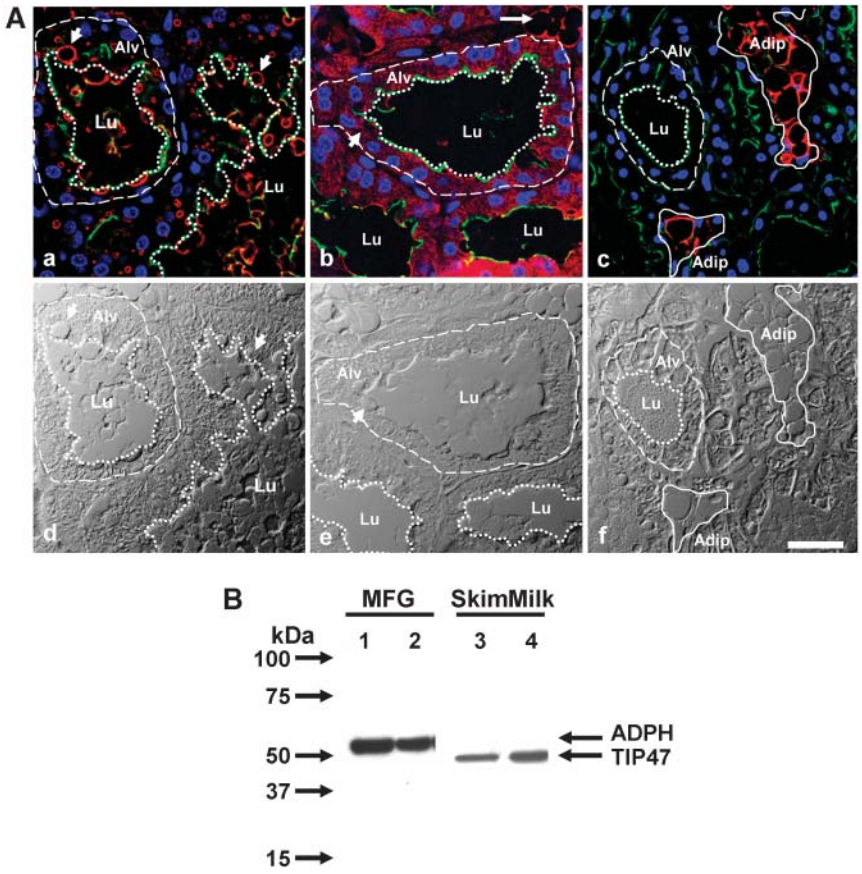

Fig. 1. PAT proteins differ in their localization in lactating mouse mammary tissue. A: Mammary tissue sections from day 10 lactating mice were immunostained with antibodies to adipophilin (ADPH) (a), TIP47 (b), or perilipin (c) and Alexa Fluor® 594-conjugated secondary antibodies. Differential interference contrast images (d–f) of each section are shown to indicate relationships between structural features of the mammary gland and immunofluorescence staining patterns. Individual alveoli (Alv) are enclosed by dashed lines. Alveolar lumens (Lu) are indicated by dotted lines and were identified by staining with Alexa Fluor® 488-WGA. Adipose tissue (Adip) is indicated by solid lines. Nuclei were stained with 4′,6-diamidino-2-phenylindole. Arrowheads indicate cytoplasmic lipid droplets (CLDs). The arrow indicates TIP47 staining in adipose tissue. Bar = 50 μm. B: Immunoblot analysis of ADPH and TIP47 in the milk fat globules (MFGs) and skim milk fractions of mouse milk. Milk from two mice was fractionated into MFGs (lanes 1, 2) and skim milk fractions (lanes 3, 4).

ciated with cytoplasmic and secreted lipid droplets in lactating mouse mammary epithelial cells.

ADPH selectively localizes to CLDs in differentiating alveolar epithelial cells

Mammary gland differentiation in mice is initiated around mid pregnancy (gestation in our colony is 19–20 days) with the formation and growth of alveoli (7, 45). As described previously (7, 45, 46), in the beginning of this process the mammary gland is composed mostly of adipose cells with a few small alveoli that both lack discrete luminal regions and have no readily visible CLDs (**Fig. 2A**). Around mid pregnancy, alveoli have increased in number and size; however, the mammary gland is still composed predominantly of adipose cells (Fig. 2B). Toward the end of pregnancy [postcoital day 17 (PCD17)], numerous clusters of alveoli, many of which contain numerous prominent CLDs, are present in mammary tissue (Fig. 2C). Although adipose tissue is still present at this stage, alveoli are now prominent components of the mouse mammary gland. Within 24 h after parturition and the initiation of milk secretion (PCD20), the adipose tissue component is markedly reduced and there is significant expansion of alveoli, which now have large luminal regions. At this stage, large CLDs are no longer readily visible in alveoli (Fig. 2D), but secreted MFGs can be observed in lumens at higher power (data not shown).

To better understand CLD accumulation in differentiating mammary alveoli and determine whether ADPH and/or TIP47 is involved in this process, mammary tissue sections were obtained from pregnant and lactating mice at closely spaced developmental intervals and stained for ADPH and TIP47 (**Fig. 3**). Figure 3A (panel a) shows that small ADPH-positive CLDs were detected in some alveolar epithelial cells as early as PCD7. Between PCD7 and PCD12 (Fig. 3A, panel b), ADPH-positive CLDs remained

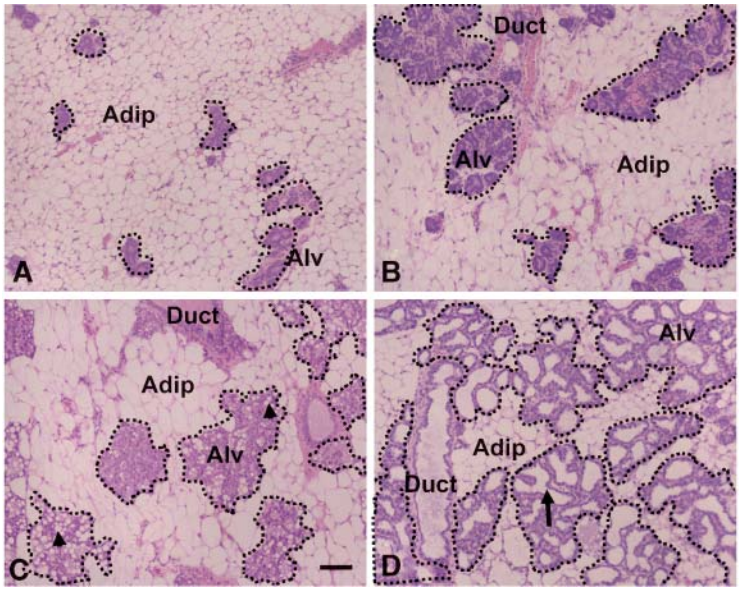

Fig. 2. Histological changes in the differentiating mammary gland. Low-power images of hematoxylin and eosin-stained sections of mammary tissue from pregnant and lactating mice show the growth of alveolar structures and the accumulation of CLDs in secretory epithelial cells in late pregnancy. A: Postcoital day 3 (PCD3). B: PCD12. C: PCD17. D: PCD20 (lactation day 2). Alveolar regions are outlined by dotted lines. Alveolar (Alv) and adipose (Adip) tissue and ducts are indicated. Arrowheads indicate CLDs, and the arrow indicates the alveolar lumen. Bar = 100 μm.

relatively small and many alveolar epithelial cells lacked these structures. In addition, there was considerable cell-cell variability in the number and size of ADPH-positive CLDs within individual cells. Beginning around PCD14, larger ADPH-positive CLDs began to accumulate in some cells (Fig. 3A, panel c). At this stage, however, there was still significant variability in CLD size and number and many cells still lacked these structures. By PCD16, nearly all cells possessed ADPH-positive CLDs, and in some cells these CLDs had diameters in the 10 μm range (Fig. 3A, panel d). By PCD18, the cytoplasm of alveolar epithelial cells appeared to be completely filled with large ADPH-positive CLDs, many of which had diameters in excess of 10 μm (Fig. 3A, panel e). Within 24 h after parturition and the onset of lactation (PCD20), numerous small ADPH-positive CLDs were observed to be enriched along the apical border of alveolar epithelial cells (Fig. 3A, panel f). These changes appeared to be related specifically to alveolar differentiation, as ADPH-positive CLDs were not detected in ductal epithelial cells during pregnancy and only small numbers of positive CLDs were detected in some ductal cells of lactating animals (Fig. 3B). In addition, the absence of ADPH immunofluorescence in nonepithelial compartments of the mammary gland (Fig. 3A, B) indicates that it is not found in mammary adipocytes from pregnant or lactating animals. Together, these results suggest that ADPH is primarily a secretory epithelium-specific protein in the mouse mammary gland.

TIP47 was also detected in differentiating alveolar epithelial cells by immunofluorescence (Fig. 3C). However, rather than being associated with CLDs, like ADPH, it had a diffuse cytoplasmic staining pattern. Moreover, TIP47 appeared to be present in all alveolar epithelial cells, even during the early stages of differentiation (Fig. 3C, panel a). In addition, there did not appear to be any enrichment of TIP47 along the apical border of these cells once lactation was initiated (Fig. 3C, panel d). These data suggest that TIP47 is not normally associated with CLDs in alveolar epithelial cells either during differentiation or in their mature milk-secreting state.

ADPH expression and CLD accumulation are developmentally linked during mammary gland differentiation

The results in Fig. 3 suggest that CLD accumulation in alveolar epithelial cells follows a specific developmental pattern during secretory differentiation. To better define this developmental pattern, we quantified CLD size in differentiating and lactating alveoli. **Figure 4A** shows that CLD size increased modestly between PCD7 and PCD16; however, the sharpest increase in CLD size occurred near the end of pregnancy, when between PCD17 and PCD18 the average CLD size increased to 6 μm. However, once milk secretion was initiated, CLD size decreased dramatically. Figure 4A shows that within 24 h after parturition, the average CLD size was only one-sixth that of PCD18 values. These results suggest that CLD size is influenced by the balance between their rates of formation and secretion.

The immunofluorescence data in Fig. 3 predict that ADPH levels in differentiating mammary tissue will correlate with changes in CLD accumulation. In agreement with this prediction, immunoblot analysis demonstrated that mammary gland levels of ADPH protein increase with changes in CLD size and number during differentiation and decrease somewhat after the initiation of lactation and lipid secretion (Fig. 4B). In contrast, we found that TIP47 levels were not temporally correlated with CLD accumulation during these periods (Fig. 4B). These data suggest that CLD accumulation in alveolar epithelial cells is developmentally linked to increased ADPH expression. However, ADPH is known to be stabilized by association with triglycerides in CLDs and to undergo rapid proteasome-mediated degradation in the absence of triglyceride synthesis (47). This being the case, changes in ADPH levels

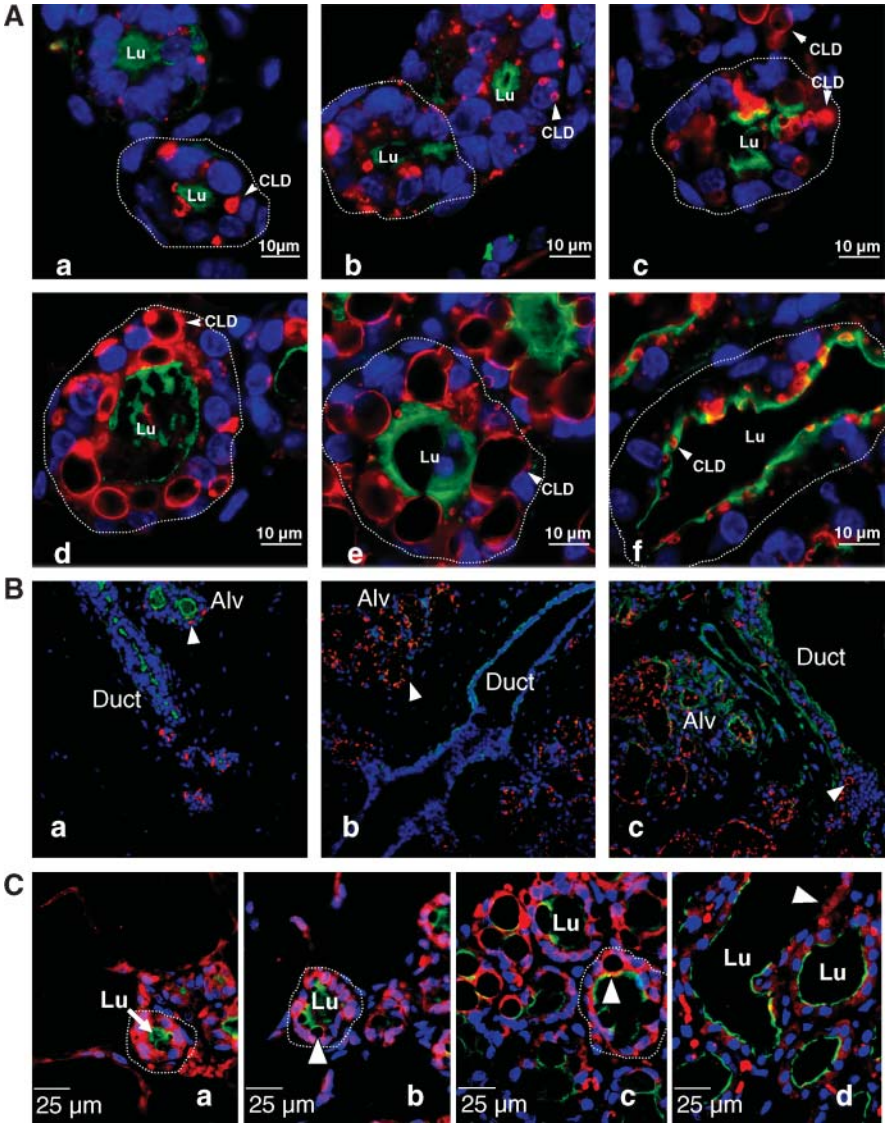

Fig. 3. ADPH and TIP47 differ in localization in the differentiating mammary gland. A: Immunolocalization of ADPH (red) in differentiating and lactating mouse mammary tissue. Higher power images at PCD7 (a), PCD12 (b), PCD14 (c), PCD16 (d), PCD18 (e), and PCD20 (day 2 of lactation) (f) show that ADPH (red) specifically localizes to CLD (arrowheads, panels a–e) in epithelial cells in differentiating and mature alveoli. Note that ADPH-coated CLDs increase markedly in size during the last half of pregnancy. After the onset of lactation, ADPH-coated CLDs concentrate at the apical membrane (arrowhead, panel f). B: Lower power images show the absence of ADPH-stained CLDs in ductal epithelial cells at days 14 (a) and 18 (b) of pregnancy. Limited numbers of small CLDs were observed in ductal epithelial cells on lactation day 2 (arrowhead, panel c). C: Immunolocalization of TIP47 (red) in differentiating mouse mammary tissue. Higher power images of alveolar epithelial cells at PCD12 (a), PCD16 (b), PCD18 (c), and PCD20 (d) show that, in contrast to ADPH, TIP47 localizes diffusely within the cytoplasm of epithelial cells of developing and mature alveoli but is not enriched around CLDs (arrowheads). Alveoli are indicated by dotted lines in A and C. Apical borders of alveoli were identified by Alexa Fluor® 488-WGA staining (green). Nuclei (blue) were stained with DAPI. Alveoli (Alv) and alveolar lumens (Lu) are indicated.

could simply reflect posttranslational stabilization of ADPH by CLDs or diminished proteasomal activity. Although analysis of specific proteasomal activity is difficult in complex tissues such as the mammary gland, we previously observed that genes encoding components of the 26S proteasome complex did not change significantly during pregnancy (48). In addition, we found little change in the pattern of ubiquitinated proteins in mammary tissue extracts during this period (data not shown). Together, these results suggest that generalized decreases in proteasomal activity are not responsible for increases in ADPH protein levels during mammary gland differentiation. To determine whether ADPH transcript levels increase during mammary gland differentiation, we quantified steady-state

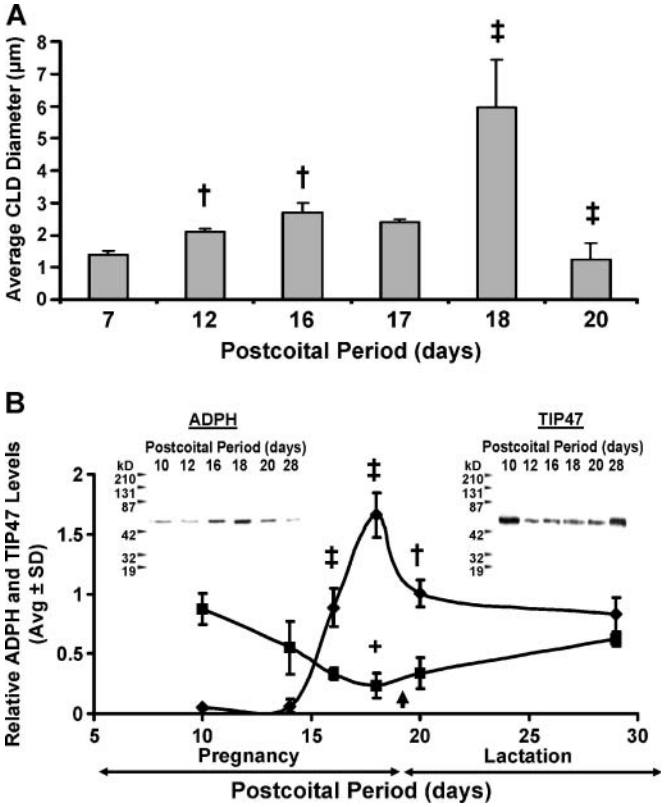

Fig. 4. ADPH protein levels correlate with CLD size and accumulation. A: Change in CLD diameter in secretory epithelial cells at the indicated days of pregnancy (PCD7–PCD18) and lactation (PCD20, L2). The values are average diameters (μm) ± SEM determined from an analysis of individual CLDs in 30–60 randomly chosen alveoli from three sections per animal. Three animals were analyzed per time point. † The value was significantly different from the value of the preceding time point ($P < 0.01$); ‡ the value was significantly different from the value of the preceding time point ($P < 0001$). B: Relative changes in ADPH (diamonds) and TIP47 (squares) protein levels in mammary tissue at the indicated days after coitus were determined by immunoblot analysis and quantified by densitometry. The values are average (±SEM) densitometric measurements normalized to β-actin from three to four animals per time point. Representative immunoblot analyses for each protein are shown in the insets. Immunoblot analyses of tissue extracts were performed twice with similar results. ‡ the value was significantly different from the value of the preceding time point for ADPH ($P < 0.00001$); † the value was significantly different from the value of the preceding time point for ADPH ($P < 0.001$); + the PCD18 value was significantly different from the PCD10 and PCD28 values for TIP47 ($P < 0.001$). Pregnancy and lactation periods are indicated by double-headed horizontal arrows. Parturition is indicated by the up arrow.

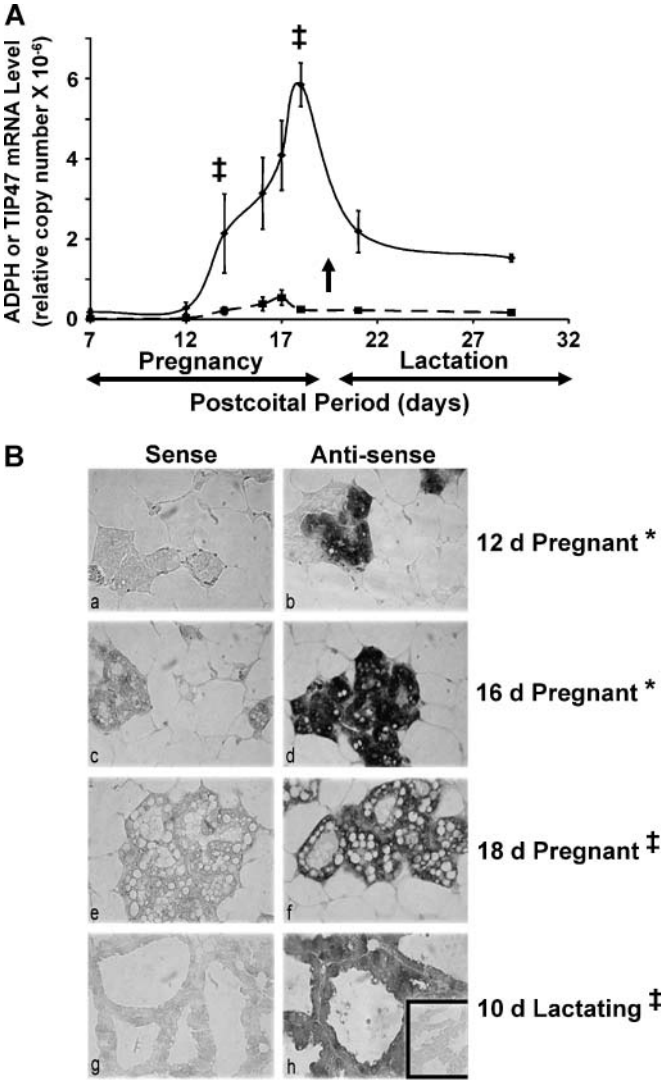

Fig. 5. Induction of ADPH expression during pregnancy. A: Developmental changes of ADPH (solid line) and TIP47 (dashed line) mRNA copy numbers as assessed by quantitative real-time PCR (QRT-PCR). Values are average copy numbers (±SEM) normalized to β-2-microglobulin for three to four animals per time point. Pregnancy and lactation periods are indicated by horizontal double-headed arrows. The up arrow indicates the time of parturition.‡ The PCD18 value was significantly different from the PCD14 value ($P < 0.005$). B: In situ hybridization of ADPH in mammary tissue sections from mice at pregnancy days 12, 16, and 18 and lactation day 10. Tissues in panels a, c, e, and g were labeled with digoxigenin-conjugated sense oligonucleotides to mouse ADPH. Tissues in panels b, d, f, and h were labeled with digoxigenin-conjugated antisense oligonucleotides to mouse ADPH. The inset in panel h shows the lack of reaction in tissues treated with RNase before in situ hybridization with antisense oligonucleotides. Tissue sections were incubated for 5 h with substrate (asterisks) or for 1 h with substrate (double daggers). Note the uniform staining of alveoli and the lack of adipose staining under these conditions.

levels of ADPH mRNA between PCD7 and PCD29 (lactation day 10) using QRT-PCR. **Figure 5A** shows that, like ADPH protein, steady-state levels of ADPH mRNA increased dramatically during the last half of pregnancy and reached a peak at PCD18. However, the largest increase in ADPH mRNA occurred between PCD12 and PCD14, before the detection of increases in ADPH protein or CLD number. The expression of TIP47 was also increased between PCD12 and PCD14; however, steady-state levels of TIP47 mRNA peaked at PCD17 and were >1 order of magnitude lower than those of ADPH throughout pregnancy and lactation.

Although these results are consistent with the concept that ADPH expression is increased during the differentiation of alveolar epithelial cells, this interpretation is

complicated by changes in the relative proportions of epithelium and adipose tissue in the differentiating mammary gland and by observations that ADPH transcripts are expressed in mature adipocytes in culture (16, 23). To determine which cell types express ADPH transcripts, and to verify that ADPH transcript expression increases in differentiating secretory epithelial cells, sections of mammary tissue from pregnant and lactating mice were analyzed by in situ hybridization using ADPH-specific probes. Figure 5B shows that ADPH transcripts are detected selectively in alveolar epithelial cells in both differentiating and mature mammary glands. In contrast to the significant cell-cell variability observed in ADPH-positive CLDs in these cells during the initial phases of mammary gland differentiation (Fig. 3A), there appeared to be little or no cell-cell variability in ADPH transcript expression during the differentiation process. These observations confirm that ADPH expression is increased selectively in alveolar epithelial cells during mammary gland differentiation and are consistent with the concept that increased ADPH expression promotes CLD accumulation in these cells. However, differences in the temporal patterns of ADPH transcript expression and CLD accumulation suggest that other factors contribute to this process.

Lipid metabolism is altered in the differentiating mammary gland

Changes in fatty acid availability and/or lipid metabolism are also potential regulators of CLD accumulation. The lipid content of the mammary gland adipose stores begins to be depleted in late pregnancy and is significantly depleted in response to lactation (49, 50). It has been postulated that this depletion of adipose lipid is attributable to shunting of fatty acids into secretory epithelial cells for milk lipid synthesis (51). To determine whether functional relationships exist between adipose lipid storage capacity and CLD accumulation in differentiating secretory epithelial cells, we characterized perilipin protein and mRNA levels in differentiating mammary tissue. Immunofluorescence staining (**Fig. 6A**) shows that there is a decrease in perilipin-positive adipose cells during mammary gland differentiation and that adipose cells adjacent to differentiating alveoli have a shrunken appearance. Immunoblot (Fig. 6B) and QRT-PCR (Fig. 6C) analyses of differentiat-

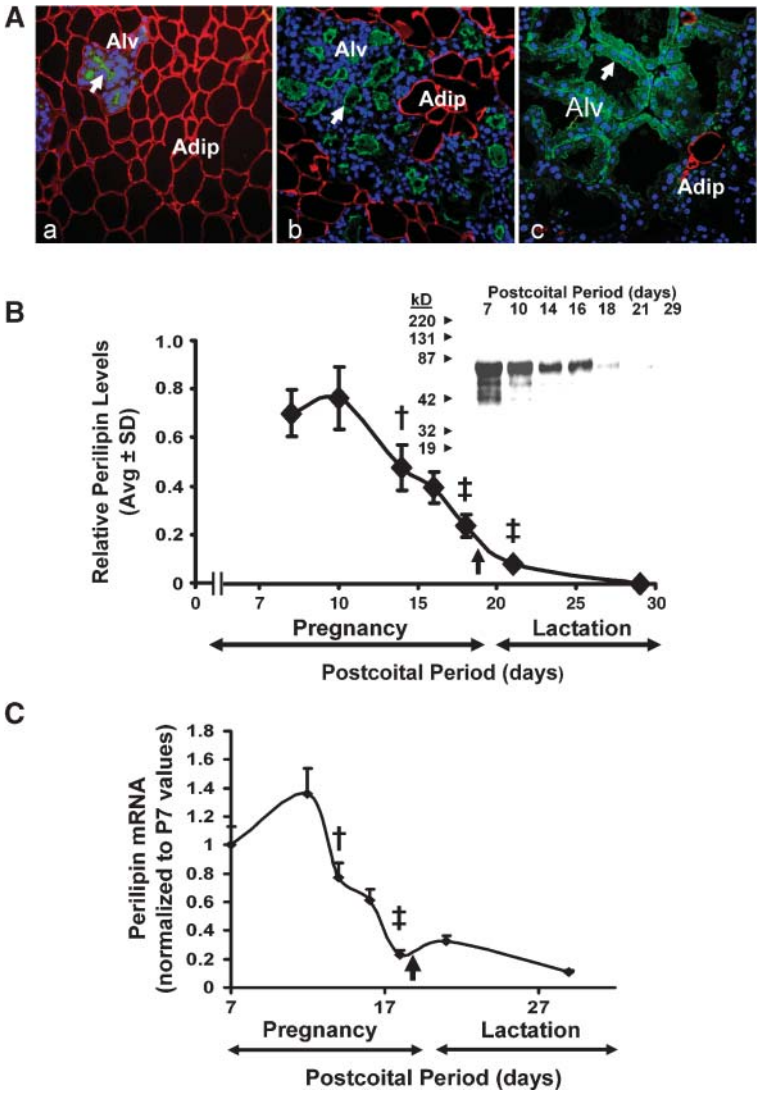

Fig. 6. Perilipin levels decrease during mammary gland differentiation. A: Immunofluorescence analysis of perilipin (red) in mammary gland sections showing depletion of perilipin-positive adipose cells (Adip) in differentiating and lactating mammary glands at PCD7 (a), PCD17 (b), and PCD20 (lactation day 2) (c). Alveoli (Alv) were identified by staining their luminal borders (arrow) with Alexa Fluor® 488-WGA (green). Nuclei (blue) were stained with DAPI. Note that the number of perilipin-positive adipose cells in mammary tissue declines dramatically during pregnancy and lactation. B: Change in relative steady-state perilipin protein levels in mammary tissue at the indicated times after coitus. Perilipin protein was determined by immunoblot analysis (inset) and quantified by densitometry. The values are average (±SEM) densitometric measurements normalized to β-actin from three to four animals per time point. † The value was significantly different from the value of the preceding time point ($P < 0.05$); ‡ the value was significantly different from the value of the preceding time point ($P < 0.01$). Error bars for PCD21 and PCD29 values are within the size of the symbol. C: Change in steady-state levels of perilipin mRNA in mouse mammary tissue during pregnancy and lactation. Relative perilipin mRNA was determined by QRT-PCR. Values are normalized to PCD7 values and are averages ± SEM for three to four animals per time point. † The value was significantly different from the previous value ($P < 0.01$); ‡ the value was significantly different from the previous value ($P < 0.005$). Pregnancy and lactation periods are indicated in B and C by double-headed horizontal arrows. Up arrows indicate the time of parturition.

ing mammary tissue show that perilipin protein relative to tissue actin and mRNA relative to total RNA begin to decrease about mid pregnancy, and by the end of pregnancy (PCD18), relative perilipin protein and mRNA levels are only 25% and 14%, respectively, of their mid pregnancy values (PCD10). The temporal correlation between the decline in perilipin expression and the increase in ADPH expression in secretory epithelial cells is consistent with the possibility that the processes are functionally linked and suggest that reduced lipid storage capacity by mammary adipose may contribute to enhanced lipid accumulation in differentiating secretory epithelial cells.

In previously published studies, we reported changes in the expression of lipid metabolism genes in mouse mammary glands during pregnancy and in lactation from microarray analysis of FVB mice, finding that these changes were consistent with those from another laboratory in C57Bl6 mice (48, 52, 53). In limited microarray analyses on the CD1 mouse strain used for these studies, we again found comparable changes in lipid metabolism gene expression between late pregnancy and early lactation (data not shown). For this reason, we are comfortable that the results of the analysis of three genes involved in lipid synthesis, whose expression is likely limited in adipose tissue, are representative of changes in the epithelial compartment only of most if not all mouse strains. These genes are Glut1 (gene accession number M22998), the major glucose transporter in the mammary epithelium (54), and a Δ5 fatty acid desaturase (Fads1; gene accession number AK083959) and a fatty acid elongase (Elovl1; gene accession number AI842813) that likely contribute to the desaturation and elongation of fatty acids in the mammary gland to produce the long-chain polyunsaturated fatty acids characteristic of milk (53). The expression patterns of these genes are consistent (**Fig. 7**). Starting after PCD7, there is a slow 2-fold increase in expression, followed by a 2- to 3-fold increase between PCD17 and PCD20 (lactation day 2). These observations suggest that there is a slow upregulation of the genes of lipid synthesis in the mammary epithelium during late pregnancy that contributes to CLD accumulation.

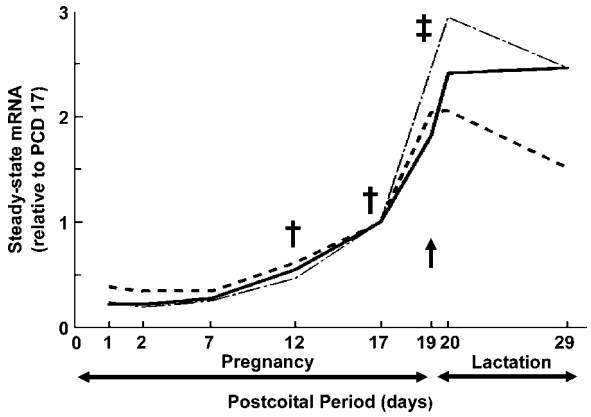

Fig. 7. Expression of genes contributing to lipid synthesis in mouse mammary glands during pregnancy and lactation. Relative expression levels of Glut-1 (solid line), Δ5 fatty acid desaturase (mixed dashed line), and fatty acid elongase (dashed line) in differentiating mouse mammary tissue are shown. Values are means from analysis of four mice per time point. Standard errors, not shown, were <10% of the mean. † The value was significantly different from the preceding value ($P < 0.01$); ‡ the value was significantly different from the preceding value ($P < 0.005$).

DISCUSSION

The stabilization of nascent CLDs by PAT proteins is thought to be an important element in their accumulation (55). Our study provides evidence that ADPH mediates CLD accumulation in differentiating secretory epithelial cells in the mouse mammary gland. The observations that both CLD accumulation and ADPH expression selectively increase in these cells during their differentiation suggest that they are specific, developmentally induced properties of the secretory epithelium. Although TIP47 can localize to CLDs (56–58) and there have been reports that it is found on MFGs in human milk (22, 42), our data indicate that it is not associated with CLDs in milk-secreting cells of the mouse mammary gland and is not a component of secreted MFGs. Interestingly, our immunofluorescence results indicate that, like ADPH, TIP47 is enriched in secretory epithelial cells, which suggests that it may be important for their differentiation or function. However, observations that TIP47 levels are inversely correlated with CLD levels in these cells argue against a role for it in CLD accumulation or secretion in the normal mouse mammary gland. At present, it is unclear whether the presence of TIP47 in MFGs from human milk (22) reflects species differences in the types of PAT proteins associated with CLDs or whether other mechanisms are involved. For instance, it is known that MFGs in some species, including humans, possess significant amounts of cytoplasmic inclusions, which can contain endoplasmic reticulum and Golgi fragments (7). Because TIP47 normally functions as an adaptor protein in endocytic vesicle trafficking (21), it is possible that vesicular material containing TIP47 becomes trapped during MFG formation in humans but not in mice. Interestingly, we found TIP47 in skim milk fractions, which also suggests that mechanisms exist for its transfer into milk independent of milk lipid secretion. Although it is unclear how this transfer occurs, skim milk fractions are known to contain small membrane vesicles (7), and it is possible that TIP47 is transferred into milk in association with this material.

CLD accumulation in secretory epithelial cells was long ago observed to be initiated during pregnancy and associated with the differentiation of the mammary gland into a secretory organ (7, 45); however, the factors regulating this process were poorly defined. Our data show that the accumulation and growth of these structures correspond to increased ADPH expression and follow a distinct biphasic developmental pattern. In agreement with earlier histological and electron microscopy studies (7, 45), we found that only limited numbers of secretory epithelial cells possessed ADPH-positive CLDs during the initial phase of differentiation (PCD7–PCD14) and that among

these cells there was considerable cell-cell variability in both the number and size of CLDs. The observation that ADPH transcripts appear to be expressed uniformly in all secretory epithelial cells, even those that lack visible CLDs, suggests that differences in ADPH expression are not the cause of cell-cell variability in CLD accumulation. Importantly, the presence of ADPH mRNA in cells before the appearance of CLDs suggests that ADPH expression may be one initiating event in CLD accumulation. However, the significant lag between the increase in ADPH mRNA and the increase in CLD accumulation indicates that increased ADPH expression is not the only factor driving this process.

The possibility that developmental increases in the lipid synthetic capacity of secretory epithelial cells contribute to CLD accumulation was suggested by studies showing that lipid synthetic activity increases in differentiating mouse mammary tissue in late pregnancy (59). More recently, array studies have demonstrated widespread changes in the expression of genes involved in lipid metabolism at the end of pregnancy (48, 53). Furthermore, the array data presented here show an increase in epithelium-specific genes that contribute to the synthesis of milk lipid that is temporally similar to changes in CLD accumulation. Together, these data are consistent with developmentally driven increases in lipid production in differentiating secretory epithelial cells, which may contribute to CLD accumulation.

In addition to alterations in secretory epithelial cell lipid metabolism, our data also indicate that diminished lipid storage in mammary adipocytes may contribute to CLD accumulation by shunting of fatty acids to secretory epithelial cells. Loss of perilipin is known to decrease triglyceride storage in adipose cells and to increase serum fatty acid levels (60, 61). Our observations that relative perilipin protein and mRNA levels decrease with a time course similar to that of CLD accumulation in differentiating secretory cells suggest that the two processes may be functionally related. Indeed, earlier studies documented that depletion of lipid in mammary adipose cells during late pregnancy and lactation is dependent on the presence of an epithelial component (49). In this context, it is interesting that steady-state levels of perilipin protein and mRNA begin to decrease at mid pregnancy, well before alveoli are significant cellular components of the mammary gland. Thus, it is unlikely that declines in perilipin expression are attributable simply to displacement of the adipose compartment by alveoli (49). At present, the factors regulating adipose lipid depletion and the reduction of perilipin expression are not well defined, but both systemic hormones and/or epithelium-derived paracrine factors are possible contributors. Collectively, our data suggest that CLD accumulation in the differentiating mouse mammary gland is a sequentially ordered process that is initiated around mid pregnancy by increased expression of ADPH, which functions to stabilize the triglyceride core in nascent CLDs. Subsequent CLD accumulation is proposed to depend on increases in intracellular fatty acid levels, which are likely to be driven by both increased de novo fatty synthesis in secretory epithelial cells and reduced lipid storage by adipose cells.

In summary, previous studies of mammary gland differentiation have focused primarily on changes in genetic or biochemical markers, and little was known about the cell biological aspects of this process. Our data provide evidence that CLD accumulation and trafficking are prominent features of the differentiating mammary gland and appear to be early and specific markers of the differentiation process. We previously demonstrated that ADPH specifically colocalizes with xanthine oxidoreductase and butyrophilin at sites of CLD secretion on apical membranes of secretory epithelial cells in lactating mouse mammary glands and exists as a stable complex with these proteins on isolated MFGs (35). Together, these observations raise the possibility that ADPH functions in both the formation and secretion of CLD by mammary epithelial cells. Although recent freeze-fracture localization studies have raised questions about the exact role of ADPH in CLD secretion (42), they nevertheless demonstrate an enrichment of ADPH on the apical membrane at sites that contact CLDs, which is consistent with the possibility that ADPH contributes to interactions between CLDs and the apical plasma membrane.

Whether or not this interaction is caused by a specific association with a xanthine oxidoreductase-butyrophilin complex, as hypothesized previously (6, 35), the ability of ADPH to associate with the CLD surface as well as with the plasma membrane implies that it possesses distinct binding functions (5). Previous studies have identified CLD targeting regions in the N-terminal portion of ADPH (33, 62), and it will be important to define the in vivo roles of these, as well as other, regions of the ADPH molecule in the formation and secretion of CLDs. Of interest, the crystal structure of the C-terminal region of TIP-47, which is structurally similar to that of ADPH, has been shown to be composed of a four helix bundle similar to the putative membrane binding domain of apolipoprotein E (63). Thus, it will be important to determine whether this structure contributes to interactions between CLD and membrane structures or other physiological functions of ADPH (5). As yet, there is relatively limited information on the physiological roles of ADPH, although recent data have shown that loss of ADPH is protective against the development of fatty liver (64). Our data suggest that the differentiating mammary gland is a useful model in which to study developmental mechanisms regulating CLD accumulation and secretion, and it will be interesting in future studies to determine how the loss of ADPH affects these processes.

This research was supported by grants from the National Institutes of Health, RO1 HD-045962 (J.L.M.) and PO1 HD-38129 (J.L.M., M.C.N.). C.A.P. was supported by National Research Service Award Postdoctoral Fellowship HD-044359. The authors thank W. Zabaronick for excellent technical assistance.

REFERENCES

1. Allen, J. C., R. P. Keller, P. C. Archer, and M. C. Neville. 1991. Studies in human lactation. VI. Milk composition and daily secre-

tion rates of macronutrients in the first year of lactation. *Am. J. Clin. Nutr.* **54:** 69–80.
2. Schwertfeger, K. L., J. L. McManaman, C. A. Palmer, M. C. Neville, and S. M. Anderson. 2003. Expression of constitutively activated Akt in the mammary gland leads to excess lipid synthesis during pregnancy and lactation. *J. Lipid Res.* **44:** 1100–1112.
3. Neville, M. C., J. Morton, and S. Umemora. 2001. Lactogenesis: the transition from pregnancy to lactation. *Pediatr. Clin. North Am.* **48:** 35–52.
4. Neville, M. C., and C. W. Daniel. 1987. The Mammary Gland: Development, Regulation and Function. Plenum Press, New York.
5. McManaman, J. L., M. E. Reyland, and E. C. Thrower. 2006. Secretion and fluid transport mechanisms in the mammary gland: comparisons with the exocrine pancreas and the salivary gland. *J. Mammary Gland Biol. Neoplasia.* **11:** 249–268.
6. Mather, I. H., and T. W. Keenan. 1998. Origin and secretion of milk lipids. *J. Mammary Gland Biol. Neoplasia.* **3:** 259–273.
7. Hollmann, K. H. 1974. Cytology and fine structure of the mammary gland. *In* Lactation. B. L. Larson and V. R. Smith, editors. Academic Press, New York. 3–95.
8. Londos, C., D. L. Brasaemle, C. J. Schultz, J. P. Segrest, and A. R. Kimmel. 1999. Perilipins, ADRP, and other proteins that associate with intracellular neutral lipid droplets in animal cells. *Semin. Cell Dev. Biol.* **10:** 51–58.
9. Lu, X., J. Gruia-Gray, N. G. Copeland, D. J. Gilbert, N. A. Jenkins, C. Londos, and A. R. Kimmel. 2001. The murine perilipin gene: the lipid droplet-associated perilipins derive from tissue-specific, mRNA splice variants and define a gene family of ancient origin. *Mamm. Genome.* **12:** 741–749.
10. Miura, S., J. W. Gan, J. Brzostowski, M. J. Parisi, C. J. Schultz, C. Londos, B. Oliver, and A. R. Kimmel. 2002. Functional conservation for lipid storage droplet association among Perilipin, ADRP, and TIP47 (PAT)-related proteins in mammals, Drosophila, and Dictyostelium. *J. Biol. Chem.* **277:** 32253–32257.
11. Arimura, N., T. Horiba, M. Imagawa, M. Shimizu, and R. Sato. 2004. The peroxisome proliferator-activated receptor gamma regulates expression of the perilipin gene in adipocytes. *J. Biol. Chem.* **279:** 10070–10076.
12. Bertile, F., F. Criscuolo, H. Oudart, Y. Le Maho, and T. Raclot. 2003. Differences in the expression of lipolytic-related genes in rat white adipose tissues. *Biochem. Biophys. Res. Commun.* **307:** 540–546.
13. Brasaemle, D. L., G. Dolios, L. Shapiro, and R. Wang. 2004. Proteomic analysis of proteins associated with lipid droplets of basal and lipolytically stimulated 3T3-L1 adipocytes. *J. Biol. Chem.* **279:** 46835–46842.
14. Fong, T. H., C. C. Yang, A. S. Greenberg, and S. M. Wang. 2002. Immunocytochemical studies on lipid droplet-surface proteins in adrenal cells. *J. Cell. Biochem.* **86:** 432–439.
15. Greenberg, A. S., J. J. Egan, S. A. Wek, M. C. Moos, Jr., C. Londos, and A. R. Kimmel. 1993. Isolation of cDNAs for perilipins A and B: sequence and expression of lipid droplet-associated proteins of adipocytes. *Proc. Natl. Acad. Sci. USA.* **90:** 12035–12039.
16. Brasaemle, D. L., T. Barber, N. E. Wolins, G. Serrero, E. J. Blanchette-Mackie, and C. Londos. 1997. Adipose differentiation-related protein is an ubiquitously expressed lipid storage droplet-associated protein. *J. Lipid Res.* **38:** 2249–2263.
17. Heid, H. W., R. Moll, I. Schwetlick, H. R. Rackwitz, and T. W. Keenan. 1998. Adipophilin is a specific marker of lipid accumulation in diverse cell types and diseases. *Cell Tissue Res.* **294:** 309–321.
18. Carroll, K. S., J. Hanna, I. Simon, J. Krise, P. Barbero, and S. R. Pfeffer. 2001. Role of Rab9 GTPase in facilitating receptor recruitment by TIP47. *Science.* **292:** 1373–1376.
19. Bohn, H., W. Kraus, and W. Winckler. 1983. Purification and characterization of two new soluble placental tissue proteins (PP13 and PP17). *Oncodev. Biol. Med.* **4:** 343–350.
20. Than, N. G., B. Sumegi, G. N. Than, G. Kispal, and H. Bohn. 1998. Cloning and sequence analysis of cDNAs encoding human placental tissue protein 17 (PP17) variants. *Eur. J. Biochem.* **258:** 752–757.
21. Diaz, E., and S. R. Pfeffer. 1998. TIP47: a cargo selection device for mannose 6-phosphate receptor trafficking. *Cell.* **93:** 433–443.
22. Than, N. G., B. Sumegi, S. Bellyei, T. Berki, G. Szekeres, T. Janaky, A. Szigeti, H. Bohn, and G. N. Than. 2003. Lipid droplet and milk lipid globule membrane associated placental protein 17b (PP17b) is involved in apoptotic and differentiation processes of human epithelial cervical carcinoma cells. *Eur. J. Biochem.* **270:** 1176–1188.
23. Jiang, H. P., and G. Serrero. 1992. Isolation and characterization of a full-length cDNA coding for an adipose differentiation-related protein. *Proc. Natl. Acad. Sci. USA.* **89:** 7856–7860.
24. Steiner, S., D. Wahl, B. L. Mangold, R. Robison, J. Raymackers, L. Meheus, N. L. Anderson, and A. Cordier. 1996. Induction of the adipose differentiation-related protein in liver of etomoxir-treated rats. *Biochem. Biophys. Res. Commun.* **218:** 777–782.
25. Gao, J., H. Ye, and G. Serrero. 2000. Stimulation of adipose differentiation related protein (ADRP) expression in adipocyte precursors by long-chain fatty acids. *J. Cell. Physiol.* **182:** 297–302.
26. Vosper, H., L. Patel, T. L. Graham, G. A. Khoudoli, A. Hill, C. H. Macphee, I. Pinto, S. A. Smith, K. E. Suckling, C. R. Wolf, et al. 2001. The peroxisome proliferator-activated receptor delta promotes lipid accumulation in human macrophages. *J. Biol. Chem.* **276:** 44258–44265.
27. Buechler, C., M. Ritter, C. Q. Duong, E. Orso, M. Kapinsky, and G. Schmitz. 2001. Adipophilin is a sensitive marker for lipid loading in human blood monocytes. *Biochim. Biophys. Acta.* **1532:** 97–104.
28. Gupta, R. A., J. A. Brockman, P. Sarraf, T. M. Willson, and R. N. DuBois. 2001. Target genes of peroxisome proliferator-activated receptor gamma in colorectal cancer cells. *J. Biol. Chem.* **276:** 29681–29687.
29. Exil, V. J., R. L. Roberts, H. Sims, J. E. McLaughlin, R. A. Malkin, C. D. Gardner, G. Ni, J. N. Rottman, and A. W. Strauss. 2003. Very-long-chain acyl-coenzyme A dehydrogenase deficiency in mice. *Circ. Res.* **93:** 448–455.
30. Wu, C. C., K. E. Howell, M. C. Neville, J. R. Yates, 3rd, and J. L. McManaman. 2000. Proteomics reveal a link between the endoplasmic reticulum and lipid secretory mechanisms in mammary epithelial cells. *Electrophoresis.* **21:** 3470–3482.
31. Liu, P., Y. Ying, Y. Zhao, D. I. Mundy, M. Zhu, and R. G. Anderson. 2004. Chinese hamster ovary K2 cell lipid droplets appear to be metabolic organelles involved in membrane traffic. *J. Biol. Chem.* **279:** 3787–3792.
32. Imamura, M., T. Inoguchi, S. Ikuyama, S. Taniguchi, K. Kobayashi, N. Nakashima, and H. Nawata. 2002. ADRP stimulates lipid accumulation and lipid droplet formation in murine fibroblasts. *Am. J. Physiol. Endocrinol. Metab.* **283:** E775–E783.
33. McManaman, J. L., W. Zabaronick, J. Schaack, and D. J. Orlicky. 2003. Lipid droplet targeting domains of adipophilin. *J. Lipid Res.* **44:** 668–673.
34. Larigauderie, G., C. Cuaz-Perolin, A. B. Younes, C. Furman, C. Lasselin, C. Copin, M. Jaye, J. C. Fruchart, and M. Rouis. 2006. Adipophilin increases triglyceride storage in human macrophages by stimulation of biosynthesis and inhibition of beta-oxidation. *FEBS J.* **273:** 3498–3510.
35. McManaman, J. L., C. A. Palmer, R. M. Wright, and M. C. Neville. 2002. Functional regulation of xanthine oxidoreductase expression and localization in the mouse mammary gland: evidence of a role in lipid secretion. *J. Physiol.* **545:** 567–579.
36. Ogg, S. L., A. K. Weldon, L. Dobbie, A. J. Smith, and I. H. Mather. 2004. Expression of butyrophilin (Btn1a1) in lactating mammary gland is essential for the regulated secretion of milk-lipid droplets. *Proc. Natl. Acad. Sci. USA.* **101:** 10084–10089.
37. Vorbach, C., A. Scriven, and M. R. Capecchi. 2002. The housekeeping gene xanthine oxidoreductase is necessary for milk fat droplet enveloping and secretion: gene sharing in the lactating mammary gland. *Genes Dev.* **16:** 3223–3235.
38. Wessel, D., and U. I. Flugge. 1984. A method for the quantitative recovery of protein in dilute solution in the presence of detergents and lipids. *Anal. Biochem.* **138:** 141–143.
39. Drews, R., R. K. Paleyanda, T. K. Lee, R. R. Chang, A. Rehemtulla, R. J. Kaufman, W. N. Drohan, and H. Lubon. 1995. Proteolytic maturation of protein C upon engineering the mouse mammary gland to express furin. *Proc. Natl. Acad. Sci. USA.* **92:** 10462–10466.
40. Patton, S., and G. E. Huston. 1986. A method for isolation of milk fat globules. *Lipids.* **21:** 170–174.
41. Heid, H. W., M. Schnolzer, and T. W. Keenan. 1996. Adipocyte differentiation-related protein is secreted into milk as a constituent of milk lipid globule membrane. *Biochem. J.* **320:** 1025–1030.
42. Robenek, H., O. Hofnagel, I. Buers, S. Lorkowski, M. Schnoor, M. J. Robenek, H. Heid, D. Troyer, and N. J. Severs. 2006. Butyrophilin controls milk fat globule secretion. *Proc. Natl. Acad. Sci. USA.* **103:** 10385–10390.
43. Blanchette-Mackie, E. J., N. K. Dwyer, T. Barber, R. A. Coxey, T. Takeda, C. M. Rondinone, J. L. Theodorakis, A. S. Greenberg, and C. Londos. 1995. Perilipin is located on the surface layer of intracellular lipid droplets in adipocytes. *J. Lipid Res.* **36:** 1211–1226.

44. Greenberg, A. S., J. J. Egan, S. A. Wek, N. B. Garty, E. J. Blanchette-Mackie, and C. Londos. 1991. Perilipin, a major hormonally regulated adipocyte-specific phosphoprotein associated with the periphery of lipid storage droplets. *J. Biol. Chem.* **266:** 11341–11346.
45. Wooding, F. B. P. 1977. Comparative mammary fine structure. *In* Comparative Aspects of Lactation. M. Peaker, editor. Academic Press, London. 1–41.
46. Richert, M. M., K. L. Schwertfeger, J. W. Ryder, and S. M. Anderson. 2000. An atlas of mouse mammary gland development. *J. Mammary Gland Biol. Neoplasia.* **5:** 227–241.
47. Xu, G., C. Sztalryd, X. Lu, J. T. Tansey, J. Gan, H. Dorward, A. R. Kimmel, and C. Londos. 2005. Post-translational regulation of adipose differentiation-related protein by the ubiquitin/proteasome pathway. *J. Biol. Chem.* **280:** 42841–42847.
48. Rudolph, M. C., J. L. McManaman, L. Hunter, T. Phang, and M. C. Neville. 2003. Functional development of the mammary gland: use of expression profiling and trajectory clustering to reveal changes in gene expression during pregnancy, lactation, and involution. *J. Mammary Gland Biol. Neoplasia.* **8:** 287–307.
49. Elias, J. J., D. R. Pitelka, and R. C. Armstrong. 1973. Changes in fat cell morphology during lactation in the mouse. *Anat. Rec.* **177:** 533–547.
50. Neville, M. C., D. Medina, J. Monks, and R. C. Hovey. 1998. The mammary fat pad. *J. Mammary Gland Biol. Neoplasia.* **3:** 109–116.
51. Jensen, D. R., S. Gavigan, V. Sawicki, D. Witsell, R. H. Eckel, and M. C. Neville. 1994. Regulation of lipoprotein lipase activity in the mammary gland of the lactating mouse. *Biochem. J.* **298:** 321–327.
52. Stein, T., J. S. Morris, C. R. Davies, S. J. Weber-Hall, M. A. Duffy, V. J. Heath, A. K. Bell, R. K. Ferrier, G. P. Sandilands, and B. A. Gusterson. 2004. Involution of the mouse mammary gland is associated with an immune cascade and an acute-phase response, involving LBP, CD14 and STAT3. *Breast Cancer Res.* **6:** R75–R91.
53. Rudolph, M. C., J. L. McManaman, T. Phang, T. Russell, D. J. Kominsky, N. J. Serkova, T. Stein, S. M. Anderson, and M. C. Neville. 2007. Metabolic regulation in the lactating mammary gland: a lipid synthesizing machine. *Physiol. Genomics.* **28:** 323–336.
54. Burnol, A-F., A. Leturque, M. Loizeau, C. Postic, and J. Girard. 1990. Glucose transporter expression in rat mammary gland. *Biochem. J.* **270:** 277–279.
55. Murphy, D. J. 2001. The biogenesis and functions of lipid bodies in animals, plants and microorganisms. *Prog. Lipid Res.* **40:** 325–438.
56. Sztalryd, C., M. Bell, X. Lu, P. Mertz, S. Hickenbottom, B. H. Chang, L. Chan, A. R. Kimmel, and C. Londos. 2006. Functional compensation for adipose differentiation-related protein (ADFP) by TIP47 in an ADFP null embryonic cell line. *J. Biol. Chem.* **281:** 34341–34348.
57. Ohsaki, Y., T. Maeda, M. Maeda, K. Tauchi-Sato, and T. Fujimoto. 2006. Recruitment of TIP47 to lipid droplets is controlled by the putative hydrophobic cleft. *Biochem. Biophys. Res. Commun.* **347:** 279–287.
58. Wolins, N. E., B. Rubin, and D. L. Brasaemle. 2001. TIP47 associates with lipid droplets. *J. Biol. Chem.* **276:** 5101–5108.
59. Baldwin, R. L., and Y. T. Yang. 1974. Enzymatic and metabolic changes in the development of lactation. *In* Lactation. B. L. Larson and V. R. Smith, editors. Academic Press, New York. 349–407.
60. Martinez-Botas, J., J. B. Anderson, D. Tessier, A. Lapillonne, B. H. Chang, M. J. Quast, D. Gorenstein, K. H. Chen, and L. Chan. 2000. Absence of perilipin results in leanness and reverses obesity in Lepr(db/db) mice. *Nat. Genet.* **26:** 474–479.
61. Tansey, J. T., C. Sztalryd, J. Gruia-Gray, D. L. Roush, J. V. Zee, O. Gavrilova, M. L. Reitman, C. X. Deng, C. Li, A. R. Kimmel, et al. 2001. Perilipin ablation results in a lean mouse with aberrant adipocyte lipolysis, enhanced leptin production, and resistance to diet-induced obesity. *Proc. Natl. Acad. Sci. USA.* **98:** 6494–6499.
62. Targett-Adams, P., D. Chambers, S. Gledhill, R. G. Hope, J. F. Coy, A. Girod, and J. McLauchlan. 2003. Live cell analysis and targeting of the lipid droplet-binding adipocyte differentiation-related protein. *J. Biol. Chem.* **278:** 15998–16007.
63. Hickenbottom, S. J., A. R. Kimmel, C. Londos, and J. H. Hurley. 2004. Structure of a lipid droplet protein: the PAT family member TIP47. *Structure.* **12:** 1199–1207.
64. Chang, B. H., L. Li, A. Paul, S. Taniguchi, V. Nannegari, W. C. Heird, and L. Chan. 2006. Protection against fatty liver but normal adipogenesis in mice lacking adipose differentiation-related protein. *Mol. Cell. Biol.* **26:** 1063–1076.